

RESULTS FROM THE PIERRE AUGER OBSERVATORY

L. PERRONE FOR THE PIERRE AUGER COLLABORATION

Università del Salento and INFN Lecce, via per Arnesano, I-73100, Lecce, Italy

The Pierre Auger Observatory has been designed to investigate the origin and the nature of Ultra High Energy Cosmic Rays using a hybrid detection technique. It is located on a plateau in the Province of Mendoza, Argentina, and consists of a surface array of about 3000 km² overlooked by 24 air fluorescence telescopes grouped in 4 sites which together provide a powerful instrument for air shower reconstruction. The Southern site of the Auger Observatory has been completed in June 2008 and is taking data smoothly since 2004. A review of selected results is presented with the emphasis given to the measurement of energy spectrum, chemical composition and search for photons and neutrinos as primary particles.

1 Introduction

The knowledge of high energy cosmic-ray energy spectrum, arrival directions and mass composition is relevant for the understanding of radiation production and particle acceleration mechanisms in astrophysical sources as Supernovae Remnants, Active Galactic Nuclei and Gamma Rays Bursts. Despite several models have been proposed along the past years (see for example¹ for an exhaustive review on particle acceleration mechanisms in astrophysical sources), the origin of the highest energy cosmic rays is still an open issue. The observation of extensive air showers and the study of their potential for inferring the properties of primary particles is already documented in the pioneering works coming back to the forties and the sixties^{2,3}. The all particle cosmic-ray energy spectrum follows a power law over many orders of magnitude and events with energy exceeding 10²⁰ eV have been observed for more than 40 years⁴. However, since the flux is extremely low (1 particle km⁻² century⁻¹ sr⁻¹ at energy larger than 10^{19.5} eV) very large detection areas and long observation time are needed to collect a sensible number of events. At the highest energies the spectrum exhibits several interesting features with remarkable astrophysical implications. A steepening of the flux called the “knee” appears at about 10¹⁵ eV, likely due to the leakage from galaxy of charged particles. At energies larger than 10¹⁵ eV the strength of galactic magnetic field is not sufficient to confine the lightest particles within the galaxy. The KASCADE-Grande experiment⁵ measured the knee for protons and for heavier particles giving an experimental evidence of this hypothesis. A flattening of the spectrum called the “ankle” emerges at about 5·10¹⁸ eV, followed by a flux suppression at ultra high-energies. The ankle may be an indication of the transition from a galactic to an extra-galactic component, but the interpretation of this feature is still controversial. Theories describing the ankle can be roughly grouped in two classes, the ones assuming that cosmic rays are mainly protons⁶, and the others favoring a mixed composition of protons with heavier nuclei⁷. No models can exhaustively explain all the features of the spectrum or interpret them in a consistent way. Another open problem was the existence of flux suppression at energy larger than 10^{19.5} eV. This feature is called “GZK cut-off”. It was predicted as a consequence of the interaction of high-energy particles with the cosmic microwave background⁸. Other theories based on supersymmetry do expect instead a not negligible flux of ultra high-energy particles from decay of topological defects or through more exotic scenarios⁹. The flux suppression observed by the HiRes telescope¹⁰ was not confirmed by the results of the AGASA array¹¹. The two experiments used different and independent techniques, HiRes observed the longitudinal profile of air showers by measuring the fluorescence light emitted along shower propagation through the atmosphere, AGASA was a surface array measuring the arrival time of secondary particles at ground. A fast progress has been made in the last years, also due to high statistics hybrid data from the

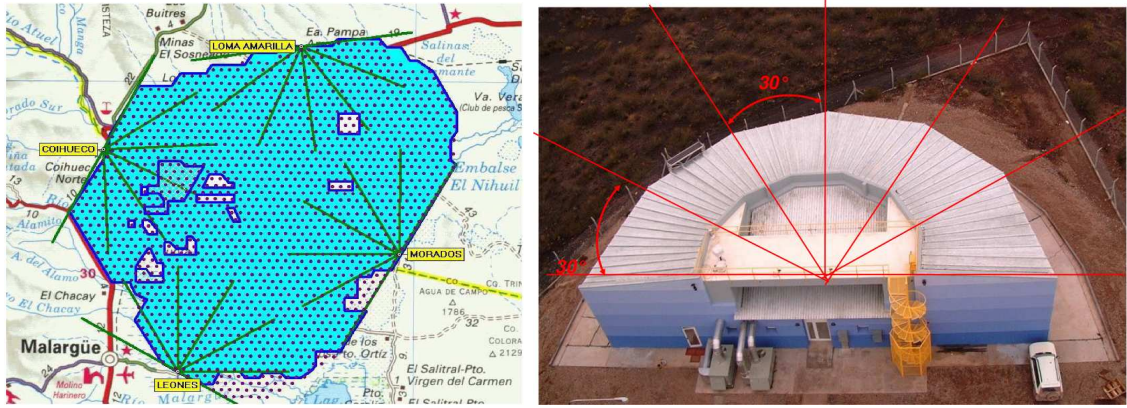


Figure 1: Layout of the Southern site of the Pierre Auger Observatory with the locations of the surface detector stations. Also shown are the locations of the fluorescence observation sites with the field of view of their telescopes. The blue region indicates the ground array currently in operation. All 24 telescopes distributed over the four sites Los Leones, Coihueco, Loma Amarilla and Los Morados are in operation. An aerial view of Los Leones site is shown on the right.

Pierre Auger Observatory. Both, the HiRes and the Pierre Auger experiments have observed a flux suppression at the highest energies as expected from the GZK-effect^{12,13}. The Pierre Auger Observatory also reported an evidence of anisotropy of the arrival directions of the highest energy events¹⁴. This result opens a completely new channel of investigation. At extremely high-energy, light charged particles are less deflected by the action of galactic and extragalactic magnetic field and they might point back to their astrophysical source. This picture would be consistent with the hypothesis that primary particles are dominated by a light component and it would nicely complement the observation of flux suppression at the highest energies. On the other hand, the measurements of atmospheric depth at shower maximum suggest rather a mixed composition with heavier nuclei¹⁵, though the interpretation of such data is much more difficult due to the strong dependence on hadronic interaction models. The puzzle is still unsolved and it is complicated by the fact that the HiRes experiment does not confirm the observation of the anisotropy¹⁶ reported by Auger. The measurement of hadronic interaction cross sections at energies four orders of magnitude larger than the ones covered by current and future accelerators is an important goal to be achieved and it would help conciliating these results. Further analyses based on shower topology have been performed searching for photons^{17,18} and neutrinos¹⁹ as primary particles. No evidence has been found for both and the derived upper limits strongly constrain several top-down and dark-matter based models originally invoked to explain the possible absence of the GZK-effect in AGASA data. The encouraging outcome of the Observatory supports the proposal of a second detector to be built in the Northern hemisphere (Colorado, USA). It would allow having a full coverage of the sky and larger statistics at the highest energies²⁰. As a final remark, new results in all the field investigated by the Pierre Auger Observatory are imminent and planned to be released by the next International Cosmic Ray Conference. At the time these proceedings will be published, they have likely been made public.

2 The Pierre Auger Observatory

The Pierre Auger Observatory employs a hybrid detection technique, allowing the reconstruction of extensive air showers with two complementary measurements. Indeed, the combination of information from the surface array and the fluorescence telescopes enhances the reconstruction capability of “hybrid” events with respect to the individual detector components. The surface

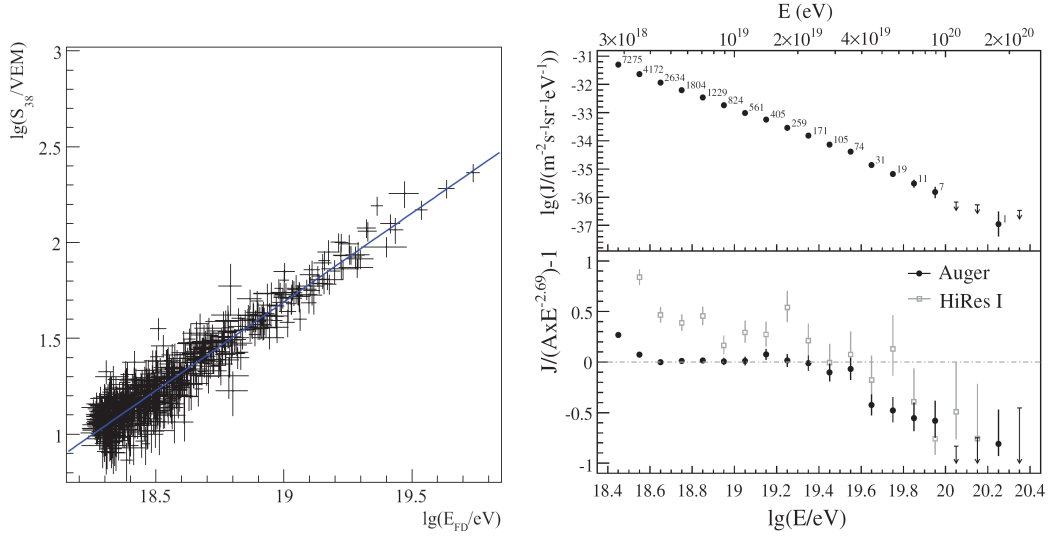


Figure 2: Left: Correlation between $\lg S_{38^\circ}$ and $\lg E_{FD}$ for the 661 hybrid events used in the fit. Right: Differential flux from the surface detector as a function of energy (top) and fractional differences between Auger and Hires I data (bottom).

detector array (SD) consists of 1600 water Cherenkov stations on a regular hexagonal grid, covering a total area of 3000 km². The stations are deployed with a spacing of 1.5 km yielding, at zenith angle less than 60°, full efficiency for extensive air shower detection above 10^{18.5} eV. The arrival direction of each event is reconstructed from the time sequence of hit stations and their signal is used to measure the lateral distribution of particles. At the edge of array, four buildings, each hosting 6 fluorescence telescopes (FD), overlook the surface detector. Each telescope consists of 440 photomultipliers placed in the focus of a 10 m² spherical mirror and observes a field of view of 30° azimuth times 30° elevation. All 24 telescopes are in operation and taking data. The fluorescence technique provides a calorimetric measurement of the primary particle energy, only weakly dependent on theoretical models through the invisible energy carried out by penetrating particles as muons and neutrinos. Despite the fluorescence yield is very low, approx. four photons per meter of electron track, large area imaging telescopes can observe the longitudinal profiles of extensive air showers during clear and moon-less (or with small moon fraction) nights allowing a duty cycle of 10-15%. The layout of the Southern site and its current status, together with an aerial view of the Los Leones fluorescence building, is depicted in Fig.1. It shows the locations of the four fluorescence detector observation sites and of the water stations in operation. Further details about the experiment and its performance can be found in Ref.²¹ The Southern site is complete. Further enhancements are being constructed including 1) an area equipped with a denser array of surface detector stations together with underground muon counters²² 2) a set of three high elevation fluorescence telescopes²³. The goal is to extend the measurement of energy spectrum and mass composition towards lower energies, down to the 0.1 EeV scale. Another important aim is to achieve a uniform full sky-coverage to allow studying global anisotropies of cosmic rays and correlations with matter concentrations in the nearby Universe. The Northern site, to be constructed in Colorado (USA), will follow soon and let fulfill these requirements.

3 Energy spectrum

A set of well reconstructed hybrid data (661 hybrid events collected in the time window between 1/1/2004 and 31/7/2007) have been used to calibrate the surface detector energy estimator

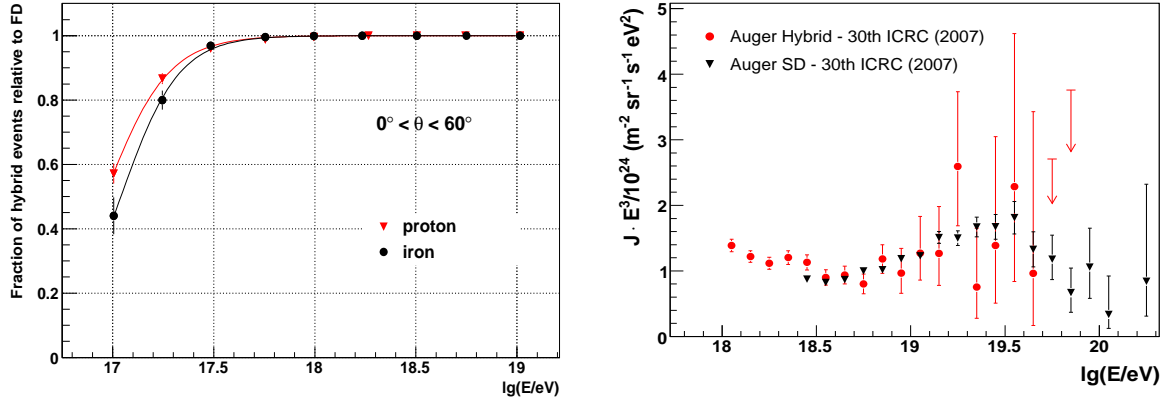


Figure 3: Left: Hybrid trigger efficiency for proton and iron. Right: Hybrid energy spectrum shown in comparison with surface detector spectrum (only statistical uncertainties are given in the figure).

S_{38° . S_{38° is the particle density at ground taken at 1000 m from shower axis if the event would had arrived with zenith angle of 38° . This calibration procedure has been designed to maximize the benefits of the surface detector (100% duty cycle and large number of events) and the fluorescence detector (quasi-unbiased calorimetric energy measurement). Only events with zenith angle less than 60° are used here. Fig. 2 (left) shows the correlation of S_{38° with the energy provided by the fluorescence detector E_{FD} . The calibration is then applied to the entire data set collected by the surface detector (about 20.000 events) and a spectrum is calculated using a SD-based geometric aperture of about 7000 km²sr y. Details of the analysis are given in ¹³. It's worthwhile reminding that the aperture used for this analysis does not depend on simulations since only events with 100% triggering probability ($E > 10^{18.5}$) are accepted. The energy spectrum is shown in Fig. 2 (right). A method which is independent of the slope of the energy spectrum is used to reject a single power-law hypothesis and a flux suppression is observed for $E > 4 \cdot 10^{19}$ eV with a significance of more than 6 standard deviations. The fractional differences between Auger and Hires I data are also shown in Fig. 2 (right). An energy shift of about 15% would result in a very good agreement between the two experiments. Given that the current estimated uncertainty on the energy scale is about 22% (dominated by the uncertainty on the fluorescence yield), results are compatible. Several measurements of the fluorescence yield have been performed in the past, e.g. the Auger Collaboration uses the fluorescence yield by Nagano et al. ²⁴ and HiRes uses the integrated yield by Kakimoto et al. ²⁵ and the spectral distribution by Bunner ²⁶. Major international efforts have been started to remeasure the fluorescence yield as a function of temperature, pressure and humidity with high precision ²⁷ in order to reduce this source of uncertainty. Hybrid data collected between December 2004 and February 2007 have been used to extend the spectrum at energy below $10^{18.5}$ eV ²⁸ in the region where the transition from Galactic to extra-galactic cosmic rays is expected to occur. Due to construction, the configuration of fluorescence telescopes and surface detector has evolved significantly and the effective detection area has correspondingly changed. The key points of this analysis are an accurate estimate of the hybrid detector exposure taking into account the exact working conditions of the experiment and an appropriate selection of well-reconstructed events. A full hybrid simulation with CORSIKA showers ²⁹ (FD and SD response are simultaneously and fully simulated) has shown that the hybrid trigger efficiency (a fluorescence event in coincidence with at least one station) is flat and equal to 1 at energies greater than 10^{18} eV. This feature is shown in Fig. 3 (left). Only data with a successful hybrid geometry reconstruction are selected for calculating the hybrid spectrum. Showers that are expected to develop outside the geometrical field of view of the fluorescence detectors are also

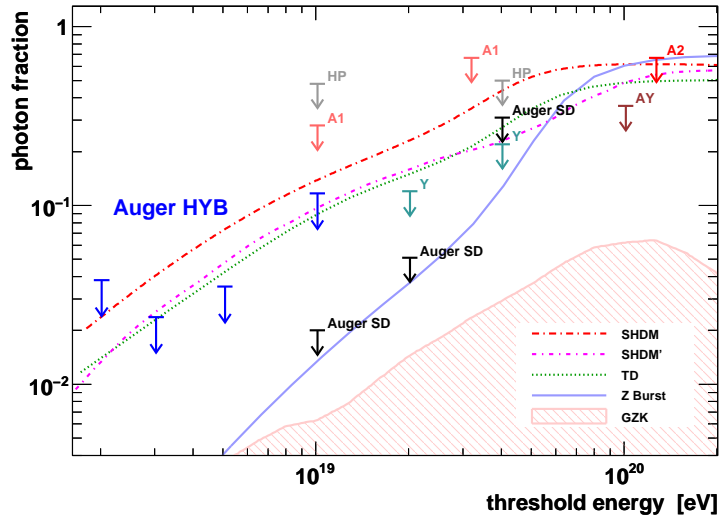


Figure 4: Upper limits on the photon fraction in the integral cosmic-ray flux for different experiments: AGASA (A1, A2), AGASA-Yakutsk (AY), Yakutsk (Y), Haverah Park (HP). In black limits from the Auger surface detector (Auger SD)¹⁷, in blue new hybrid limits above 2, 3, 5, and 10 EeV (Auger HYB)¹⁸. Lines indicate predictions from top-down models. The shaded region shows expected GZK bounds³². Figure taken from Ref.¹⁸.

rejected and, based on data, a fiducial volume for detection is defined as a function of the reconstructed energy. Exposure at the highest selection level depends very weakly on chemical composition, giving a spectrum basically independent of any assumption on primaries mass. The hybrid spectrum derived from this analysis is shown in Fig. 3 (right) compared with the spectrum from surface detector presented in³⁰ (only statistical uncertainties are given in the figure).

4 Limits on photon fraction

Primary photons can experimentally be well separated from primary hadrons as they penetrate deeper into the atmosphere, particularly at energies above 10^{18} eV. Their shower development is also much less affected by uncertainties of hadronic interaction models due to the dominant electromagnetic shower component. At the highest energies the LPM effect further delays the shower development in the atmosphere (moreover increasing shower to shower fluctuations), whereas the preshowering effect in the Earth magnetic field causes a more hadron-like behavior (see³¹ for a review on photon showers). Primary photons are of interest for several reasons: top-down models, originally proposed to explain the apparent absence of the GZK effect in AGASA data, predict a substantial photon flux at high energies³¹. In the presence of the GZK effect, UHE photons can also derive from the GZK process $p + \gamma_{CMB} \rightarrow p + \pi^0 \rightarrow p + \gamma\gamma$ and provide relevant information about the sources and propagation. Moreover, they can be used to obtain input to fundamental physics and EHE astronomy. Experimentally, photon showers can be identified by their longitudinal shower profile, most importantly by their deep X_{\max} position, larger curvature of shower front and low number of muons. Up to now, only upper limits could be derived from various experiments, either expressed in terms of the photon fraction or the photon flux. Figure 4 presents a compilation of present results on the photon fraction. The most stringent limits for $E > 10$ EeV are provided by the Auger surface detector¹⁷. Current top-down models appear to be ruled out by the current bounds. This result can be considered an independent confirmation of the GZK-effect seen in the energy spectrum. Observations in hybrid mode (i.e. observed by

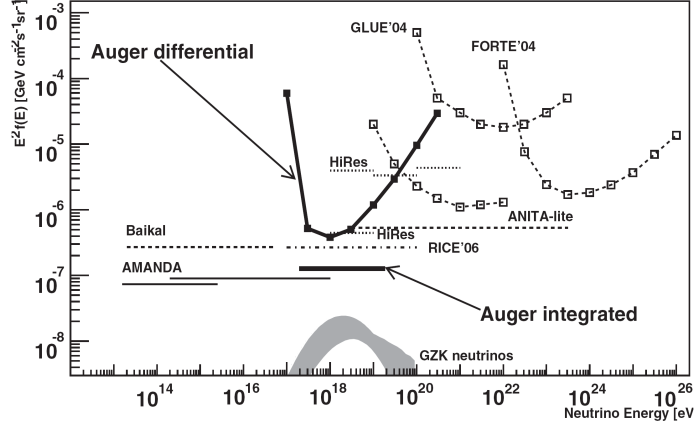


Figure 5: Limits at 90% C.L. for a diffuse flux of τ -neutrinos from the Pierre Auger Observatory. Limits from other experiments and the expected flux of cosmogenic neutrinos are also shown.

both the fluorescence and surface detectors) are also possible at energies below 10 EeV. Decreasing the energy threshold increases the event statistics, which to some extent balances the factor ~ 10 smaller duty cycle compared to observations with the ground array alone. A high quality hybrid data sample has been selected applying a set of reconstruction quality, fiducial volume and cloud cuts (see Ref. ¹⁸). The observed X_{\max} of all the photon-like events (events with large X_{\max} values) has been compared with expectations from photon-induced showers of the same geometry and energy. 8, 1, 0, 0 photon candidate events have been found with energies greater than 2, 3, 5 and 10 EeV. Their number, compatible with expectations from nuclear background, has been used to obtain an upper limit on the photon fraction in data by accounting for the corresponding cut efficiency. The limit is conservative and model independent as no nuclear background is subtracted. A detailed study of the detector efficiency as a function of energy for different primary particles has been performed. After applying all selection cuts, the acceptance for photons is close to the acceptance for nuclear primaries, and the relative abundances are preserved to a good approximation at all energies. Upper limits of 3.8%, 2.4%, 3.5% and 11.7% on the fraction of cosmic-ray photons above 2, 3, 5 and 10 EeV have been obtained at 95% C.L. Uncertainties connected to the variation of the selection cuts within the experimental resolution do not affect the derived limits. The total uncertainty in X_{\max} is $\sim 16 \text{ g cm}^{-2}$. Increasing (reducing) *all* reconstructed X_{\max} values by this amount changes the limits to 4.8% (3.8%) above 2 EeV and 3.1% (1.5%) above 3 EeV, while the limits above 5 and 10 EeV are unchanged. The new hybrid limits ¹⁸ (Auger HYB) and surface array limits ¹⁷ (Auger SD) are shown in Fig. 4 along with other experimental results, model predictions and GZK bounds ³².

5 Upper limit on the diffuse flux of ultra-high energy tau neutrinos

The detection of UHE cosmic neutrinos would open a new window to the universe. Neutrinos can result from decay of pions produced in the hadronic interaction of cosmic rays with radiation or matter in the neighbourhood of an astrophysical source. Given that neutrinos are neutral weakly interacting particles, they can travel through the Universe in straight line keeping the direction and being much less absorbed than photons and protons, thus making them a powerful and multi-tasking tool for astronomy. In addition to neutrinos of astrophysical origin and similarly to GZK-photons, GZK-neutrinos, generally called “cosmogenic neutrinos” can be produced in the interaction of high-energy cosmic rays with the microwave background. If they are produced through conventional acceleration and top-down scenarios the expected neutrino flavour ratio

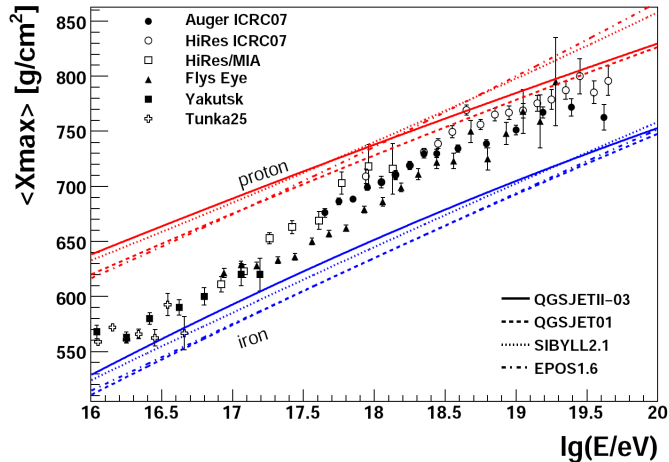


Figure 6: X_{\max} as a function of energy for Auger hybrid data¹⁵ in comparison with other experiments including HiRes³⁶. Proton and iron predictions are given for different hadronic interaction models.

at source $\nu_e : \nu_\mu : \nu_\tau$ would be 1:2:0. When propagating over astronomical distances, neutrino oscillation with maximal θ_{23} -mixing, will lead to equal numbers of ν_e, ν_μ, ν_τ . At energies above 10^{15} eV, neutrino cross sections are large enough that upgoing neutrino-induced showers cannot be detected at ground. Only τ -neutrinos entering the Earth just below the horizon (Earth-skimming) can undergo charged-current interactions in Earth's crust and produce "observable" tau leptons. Observable here means that they can travel several tens of kilometers and emerge into the atmosphere to eventually decay in flight inducing a nearly horizontal air shower with a significant electromagnetic component above the detector. Neutrino-induced air showers have a chance to be observed in ground arrays and fluorescence detectors (see e.g.³³ and references therein). A search for neutrino events has been performed using quasi-horizontal events collected by the Pierre Auger Observatory in the time between 1 January 2004 and 31 August 2007. The adopted selection criteria are based on shower footprint at ground and on time sequence of hit stations. The observation of a "young" showers (i.e. showers with a dominant electromagnetic component) arriving almost horizontally would be the signature of neutrino candidates. No evidence has been found and upper limits on the diffuse τ -neutrino flux have been derived. Assuming an E_ν^{-2} differential energy spectrum the limit set at 90% C.L. is $E_\nu^2 dN_{\nu_\tau}/dE_\nu < 1.3 \times 10^{-7} \text{ GeV cm}^{-2} \text{ s}^{-1} \text{ sr}^{-1}$ in the energy range $2 \times 10^{17} \text{ eV} < E_\nu < 2 \times 10^{19} \text{ eV}$. This is shown in Fig.5 together with other experimental results. See¹⁹ and reference therein for further details. This upper limit provides at present the best upper limit up to EeV diffuse neutrino fluxes. Similarly to the photons discussed above, they already constrain top-down models and are expected to reach the level of cosmogenic neutrinos after few years of data taking.

6 Mass Composition

Deriving the composition of cosmic rays is among the most challenging tasks in cosmic rays physics due to the fact that extensive air shower simulations need to be used for the interpretation of data. On the other hand, the chemical composition is a crucial measurement to have a consistent solution of the several still open issues related to the origin and propagation of cosmic rays. After KASCADE results³⁵, there is general consensus that the composition gets heavier above the knee³⁴. At energies above 10^{17} eV the situation is less clear, mostly because of the increasing uncertainty of the hadronic interaction models. The most robust and reliable observable to determine the primary mass in this energy range is given by the position of the shower maximum, X_{\max} , which is directly observed by fluorescence telescopes. Results from

the Pierre Auger experiment¹⁵, are shown in Fig. 6 together with a collection of available data from other experiments including HiRes³⁶. The systematic uncertainties of Auger data points are at a level of 11 g cm^{-2} at energy above 10^{18} eV and are smaller than the present uncertainties of the interaction models, particularly for proton primaries. At higher energies, the HiRes measurement yields a lighter composition than Auger which favors a mixed composition.

I would like to thank all the organizers of the EW 2009 Conference. The familiar atmosphere and the beauty of the surrounding environment made all discussions very stimulating and instructive.

References

1. M. Hillas, *Ann. Rev. Astron. Astrophys.* 22 (1984) 42.
2. P. Auger et al., *Rev Mod. Phys.* 11 (1939) 288.
3. J. Linsley and L. Scarsi, *Phys. Rev.* 128-5 (1962) 2384.
4. M. Nagano and A.A. Watson, *Rev. Mod. Phys.* 72 (2000) 689.
5. KASCADE Collaboration, *Astroparticle Physics* 24 (2005) 1.
6. V. Berezhinsky, A.Z. Gazikov and S.I. Grigorieva, *Phys. Rev. D* 74, (2006) 043005.
7. D. Allard, E. Parizot, and A. Olinto, *Astroparticle Physics*, 27 (2007), 61-75.
8. K. Greisen, *Phys. Rev. Lett.* Vol 16 (1966), 748-750. G.T.Zatsepin and V.A. Kuzmin, *JETP Lett.* Vol 4 (1966) 78-80.
9. P. Bhattacharjee and G. Sigl., *Phys. Rep.* 327 (2000) 109, 247; arXiv:astro-ph/9811011.
10. HiRes Collaboration; ArXiv Astrophysics e-prints (2007) astro-ph/0703099.
11. M. Takeda et al., *Astroparticle Physics* 19 (2003) 447.
12. R. Abbasi et al., *HiRes Coll.*, *Phys. Rev. Lett.* 100 (2008) 101101.
13. J. Abraham et al., *Pierre Auger Coll.*, *Phys. Rev. Lett.* 101 (2008) 061101.
14. J. Abraham et al., *Pierre Auger Coll.*, *Science* 318 (2007) 938.
15. M. Unger et al. *Pierre Auger Coll.*, *Proc. 30th ICRC, Merida (2007)* 4 (HE 1), 373.
16. R. Abbasi et al., *HiRes Coll.*, *Astropart. Phys.* 30 (2008) 175.
17. J. Abraham et al., *Pierre Auger Coll.*, *Astropart. Phys.* 29 (2008) 243.
18. V. Scherini, PhD-Thesis Univ. Wuppertal; J. Abraham et al. *Pierre Auger Coll.*, accepted for publication in *Astrop. Phys.* arXiv:0903.1127.
19. J. Abraham et al., *Pierre Auger Coll.*, *Phys. Rev. Lett.* 100 (2008) 211101.
20. D. Nitz et al. *Pierre Auger Coll.*, *Proc of 30th ICRC., Merida (2007)* 5 (HE 2) 889.
21. J. Abraham et al. *Pierre Auger Coll.*, *Nucl. Instr. Meth.* A523 (2004) 50.
22. A. Etchegoyen for the Pierre Auger Coll., *Proc. 30th ICRC, Merida (2007)* 5 (HE 2), 1191.
23. H. Klages for the Pierre Auger Coll., *Proc. 30th ICRC, Merida (2007)* 5 (HE 2), 849.
24. M. Nagano et al., *Astropart. Phys.* 22 (2004) 235.
25. F. Kakimoto et al., *Nucl. Instr. Meth.* A372 (1996) 527.
26. A.N. Bunner, *Cosmic Ray Detection by Atmospheric Fluorescence*, PhD Thesis, Cornell University, 1967.
27. F. Arqueros et al. *Nucl. Instrum. Meth.* A597 (2008) 1.
28. L. Perrone for the Pierre Auger Coll., *Proc. 30th ICRC, Merida (2007)* 4 (HE 1), 331.
29. D. Heck *et al*, Report FZKA 6019, (1998).
30. M. Roth for the Pierre Auger Coll., *Proc. 30th ICRC, Merida (2007)* 4 (HE 1), 327.
31. M. Risse, P. Homola, *Mod. Phys. Lett.* A22 (2007) 749.
32. G. Gelmini, O. Kalashev and D. V. Semikoz, arXiv:0706.2181 [astro-ph].
33. E. Zas, *New J. Phys.* 7 (2005) 130.
34. K.H. Kampert, *Nucl. Phys. (Proc. Suppl)* B165 (2007) 294-306; astro-ph/0611884.
35. T. Antoni et al., *KASCADE Coll.*, *Nucl. Phys. (Proc. Suppl)* B165 (2007) 294-306;
36. Y. Fedorova et al., *HiRes Coll.*, *Proc. 30th ICRC, Merida (2007)* 4 (HE 1), 463.